J|A|C|S
ARTICLES
Published on Web 08/03/2004

Persistent Photo-Reversible Transition-Metal Methylidene System Generated from Reaction of Methyl Fluoride with Laser-Ablated Zirconium Atoms and Isolated in a Solid Argon Matrix

Han-Gook Cho and Lester Andrews*

Contribution from the Department of Chemistry, P.O. Box 400319, University of Virginia, Charlottesville, Virginia 22904-4319

Received March 10, 2004; E-mail: lsa@virginia.edu

Abstract: A photoreversible transition-metal methylidene system has been formed for the first time by reaction of methyl fluoride and laser-ablated Zr atoms, isolated in solid argon, and investigated by means of infrared spectroscopy. Four different groups of absorptions are characterized on the basis of behaviors upon broad-band irradiation and sample annealing. Growth of Group I is accompanied by demise of Group II on irradiation with visible light ($\lambda > 530$ nm) and vice versa with UV light ($240 < \lambda < 380$ nm). The methylidene complex CH_2═ZrHF is responsible for Groups I and II either in different singlet−triplet spin states or argon matrix packing configurations. The ground singlet state is stabilized by an agostic interaction. On the other hand, Group III, which arises from the Grignard type compound CH_3−ZrF, disappears upon irradiation of UV light ($\lambda > 380$ nm), increasing the concentration of CH_2═ZrHF by α-H elimination. Fragments of methyl fluoride such as the CH_2F radical comprise Group IV. Theoretical calculations are carried out for the alkylidene complex and other plausible products, and the results are compared with the experimental frequencies.

Introduction

High oxidation state transition metal complexes containing a multiple metal−carbon bond were first discovered in the form of Ta alkylidenes in 1970s.[1] Since then, interest in high oxidation state alkylidene ($M{=}CR_1R_2$) and alkylidyne ($M{\equiv}CR$) species has grown dramatically, thanks to the catalytic activities of the complexes to metathesis of alkenes, alkynes, and cyclic compounds.[1−4] They are also called Schrock carbenes in honor of the discoverer and typically generated by intramolecular α-hydrogen elimination from a bis(alkyl) precursor. The transition-metal alkylidene complexes have not only provided wealth of information for the nature of metal coordination chemistry but also been regarded as one the most important ring-insertion and metathesis polymerization catalysts.[2]

Methylidenes, the simplest form of alkylidenes, provide an ideal model system to study the effects of ligands and substituent modifications. Particularly, the transition-metal methylidenes derived from simple halomethanes, inherently unstable due to lack of stabilizing resonance structures, have been the subject of recent theoretical studies.[5−9] Siegbahn and Blomberg investigated the activation of the C−H bond in methane by second row transition metal atoms and effects of halogen coordination to the metal atom and found that the reaction energy for $MX_n + CH_4 \rightarrow MX_nHCH_3$ is the largest for Zr.[5] Cundari and Gordon examined the geometry, vibrational characteristics, and electronic structures of the possible simple alkylidene complexes from halomethanes and Groups IV and V transition metal atoms.[6] Hehre also studied Group IV transition metal methylidene complexes, and found that the rotational barrier, i.e., planar−perpendicular energy differencies, is not very high (13−19 kcal/mol).[7−9] They also investigated variation in the bond lengths and hybridization in formation of the methylidenes.

It is well-known that methyl fluoride has played an important role in development of high-resolution spectroscopy in the gas phase.[10,11] Particularly, the strong absorption intensity of the ν_3 band and the coincidence with CO_2 laser lines, along with its relatively simple spectrum, have provided an ideal system for various investigations of linear and nonlinear spectroscopic phenomena. Radicals and ions related to methyl fluoride have been extensively studied as well.[12−18] The halomethane is

(1) Schrock, R. R. *Chem. Rev.* **2002**, *102*, 145.
(2) Legzdins, P.; Tran, E. *J. Am. Chem. Soc.* **1997**, *119*, 5071.
(3) Buchmeiser, M. R. *Chem. Rev.* **2000**, *100*, 1565.
(4) Choi, S.-H.; Lin, Z. *Organometallics* **1999**, *18*, 5488.
(5) Siegbahn, P. E. M.; Blomberg, M. R. A. *Organometallics* **1994**, *13*, 354, and references therein.
(6) Cundari, T. R.; Gordon, M. S. *J. Am. Chem. Soc.* **1992**, *114*, 539.
(7) Franci, M. M.; Pietro, W. J.; Hout, R. F., Jr.; Hehre, W. J. *Organometallics* **1983**, *2*, 281.
(8) Franci, M. M.; Pietro, W. J.; Hout, R. F., Jr.; Hehre, W. J. *Organometallics* **1983**, *2*, 815.
(9) Dobbs, K. D.; Hehre, W. J. *J. Am. Chem. Soc.* **1986**, *108*, 4663.
(10) Song, Q.; Schwendeman, R. H. *J. Chem. Phys.* **1993**, *98*, 9472.
(11) Feller, D.; Peterson, K. A.; de Jong, W. A.; Dixon, D. A. *J. Chem. Phys.* **2003**, *118*, 3510.
(12) Lugez, C. L.; Forney, D.; Jacox, M. E.; Irikura, K. K. *J. Chem. Phys.* **1997**, *106*, 489.
(13) Jacox, M. E.; Milligan D. E. *J. Chem. Phys.* **1969**, *50*, 3252.
(14) Andrews, L.; Dyke, J. M.; Jonathan, N.; Keddar, N.; Morris, A.; Ridha, A. *J. Phys. Chem.* **1984**, *88*, 2364.
(15) Mucha, J. A.; Jennings, D. A.; Evenson, K. M.; Hougen, J. T. *J. Mol. Spectrosc.* **1977**, *68*, 122.

dissociated by electric discharge, photolysis with vacuum UV light, or F atom reactions, and the products are studied in gas phase or in a solid rare-gas matrix.

Jacox and Milligan examined infrared spectra of the CF, HCF, and H_2CF transients by vacuum UV photolysis of methyl fluoride isolated in a solid argon matrix.[13] The vibrational characteristics of HF and $(HF)_n$ in solid argon have been investigated in this laboratory.[19,20] Hauge and Margrave studied the infrared spectra of ZrF_2, ZrF_3, and ZrF_4 provided by reaction of Zr and ZrF_4,[21] and the frequency of ZrF was predicted to be about 620 cm^{-1} by Hildenbrand and Lau.[22] The C−H insertion in hydrocarbons by laser-ablated metal atoms has been observed in various systems in our laboratory.[23−25] Particularly in a recent study, reaction of laser-ablated Zr and ethylene has been carried out, and C−H insertion products, the intermediates of H_2-elimination reaction of ethylene by the metal atom, have been identified in an argon matrix.[24] Reaction of fluorohalomethanes with alkali metal atoms have also been studied in this laboratory.[26]

In this study, reaction of laser-ablated zirconium atoms with methyl fluoride diluted in argon was carried out, and the products captured in argon matrix were investigated by means of infrared spectroscopy. Results indicate that there are at least four groups of product absorption bands on the basis of the behaviors upon photolysis and annealing, and interestingly enough, two of them consist of a persistent photoreversible system in the matrix. The vibrational characteristics of the product absorptions are confirmed by isotopic substitution and DFT calculations.

Experimental and Calculational Methods

Laser-ablated zirconium atoms (Johnson−Matthey) were reacted with CH_3F (Matheson), CD_3F (synthesized from CD_3Br and HgF_2)[14] and $^{13}CH_3F$ (MSD Isotopes, 99%) in excess argon during condensation at 7 K using a closed-cycle helium refrigerator (Air Products HC-2). The methods are described in detail elsewhere.[27−30] Concentrations of gas mixtures are typically 0.5% in argon. After reaction, infrared spectra were recorded at a resolution of 0.5 cm^{-1} using a Nicolet 550 spectrometer with an MCT detector. Samples were later irradiated by a mercury arc lamp (175 W) with optical filters, annealed to higher temperatures, and more spectra were recorded.

Complementary density functional theory (DFT) calculations were done using the Gaussian 98 package,[31] B3LYP density functional, 6-311+G(2d,p) basis sets for C, H, F, and LanL2DZ pseudopotential and basis set for Zr to provide a consistent set of vibrational frequencies for the reaction products. Geometries were fully relaxed during optimization, and the optimized geometry was confirmed via vibrational analysis. All of the vibrational frequencies were calculated analytically. In calculation of the binding energy of a metal complex, the zero-point energy is included. Complementary MP2 calculations were also performed using the SDD pseudopotential.

Table 1. Absorptions (cm^{-1}) Observed for Products of the Zr−Methyl Fluoride Reaction in Solid Argon[a]

group	CH_3F	CD_3F	$^{13}CH_3F$	
I	**1537.8**, 1532.4	**1104.3**, 1101.0	**1537.8**, 1532.7	
	742.0, **740.0**	641.8	722.9, **721.5**	
	669.4, 665.3	534.0	**664.5**, 663.7	
	633.5	607.5	632.4	
	558.7		558.0	
II	1553.0, **1551.3**	1115.3, **1114.4**	1552.7, **1551.3**	
	642.1, **631.0**	619.0	638.4, **629.1**	
	548.9	503.7		
III	1115.8	890.5	1106.4	
	611.0	610.8	610.9	
	489.2			
IV	3962.5		3962.5	(HF)[b]
	1404.6			(HCF)
	1305		1297	(CH_4)
	1278.8	1278.8	1248.6	(CF)
	1180.7	1182.9	1153.3	(HCF)
	1161.9, 1159.9	**1190.7**, 1188.5	**1139.5**, 1137	(H_2CF)
	1101			(CF_2)

[a] Stronger absorptions are bold. [b] See refs 13, 20, and 26.

Results and Discussion

The Zr and CH_3F reaction is characterized by infrared spectra of novel methylidene reaction products, which undergo reversible photochemical interconversion in the solid argon matrix. Table 1 lists the observed product frequencies.

Infrared Spectra and Photochemistry. Figure 1 shows the IR spectra in the regions of 1510−1580 and 590−760 cm^{-1} for laser-ablated Zr atoms co-deposited with Ar/CH_3F at 7 K and their variation upon photolysis and annealing. In the region of 1510−1580 cm^{-1}, strong product absorptions are found at 1532.4, 1537.8, 1551.3, and 1553.0 cm^{-1}. The ^{13}C substitution leads to negligible shifts in frequency of the absorptions, whereas deuteration results in large shifts in the frequencies as shown in Figure 2, indicating that they are all Zr−H stretching absorptions. In earlier studies, the hydrogen stretching absorptions of zirconium hydrides were observed in the same frequency region.[32,33]

Broad band Hg lamp irradiation with filter ($\lambda > 530$ nm) increases the absorptions at 1551.3 and 1553.0 cm^{-1} and decreases the absorptions at 1532.4 and 1537.8 cm^{-1}. On the other hand, irradiation using another filter ($\lambda > 290$ nm) increases both pairs of absorptions. Once they grow, the total absorbance of the absorptions stays essentially the same in the following photolysis regardless of the wavelength, whereas the ratio in intensity between the absorptions varies. Photolysis with a UV transmitting black filter ($240 < \lambda < 380$ nm) increases the absorptions at 1551.3 and 1553.0 cm^{-1} and decreases the

(16) Seccombe, D. P.; Tuckett, R. P.; Fisher, B. O. *J. Chem. Phys.* **2001**, *114*, 4074.
(17) Rosenman, E.; McKee, M. L. *J. Am. Chem. Soc.* **1997**, *119*, 9033.
(18) Nolte, J.; Wagner, H. G.; Sears, T. J.; Temps, F. *J. Mol. Spectrosc.* **1999**, *195*, 43.
(19) Andrews, L.; Johnson, G. L. *J. Phys. Chem.* **1984**, *88*, 425.
(20) Andrews, L. *J. Phys. Chem.* **1984**, *88*, 2940.
(21) Hauge, R. H.; Margrave, J. L. *High Temp. Sci.* **1973**, *5*, 89.
(22) Hildenbrand, D. L.; Lau, K. H. *J. Chem. Phys.* **1977**, *107*, 6349.
(23) Andrews, L.; Wang, X. *J. Phys. Chem. A* **2003**, *107*, 337.
(24) Cho, H.-G.; Andrews, L. *J. Phys. Chem. A* **2004**, *108*, 3965 ($Zr+C_2H_4$).
(25) Wang, X.; Andrews, L., unpublished work from this laboratory.
(26) Raymond J. I.; Andrews, L. *J. Phys. Chem.* **1971**, *75*, 3235.
(27) Burkholder, T. R.; Andrews, L. *J. Chem. Phys.* **1991**, *95*, 8697.
(28) Hassanzadeh, P.; Andrews, L. *J. Phys. Chem.* **1992**, *96*, 9177.
(29) Andrews, L.; Zhou, M. F.; Chertihin, G. V.; Bauschlicher, C. W., Jr. *J. Phys. Chem. A* **1999**, *103*, 6525.
(30) Zhou, M. F.; Andrews, L.; Bauschlicher, C. W., Jr. *Chem. Rev.* **2001**, *101*, 1931.
(31) Frisch, M. J.; Trucks, G. W.; Schlegel, H. B.; Scuseria, G. E.; Robb, M. A.; Cheeseman, J. R.; Zakrzewski, V. G.; Montgomery, Jr., J. A.; Stratmann, R. E.; Burant, J. C.; Dapprich, S.; Millam, J. M.; Daniels, A. D.; Kudin, K. N.; Strain, M. C.; Farkas, O.; Tomasi, J.; Barone, V.; Cossi, M.; Cammi, R.; Mennucci, B.; Pomelli C.,; Adamo, C.; Clifford, S.; Ochterski, J.; Petersson, G. A.; Ayala, P. Y.; Cui, Q.; Morokuma, K.; Rega, N.; Salvador, P.; Dannenberg, J. J.; Malick, D. K.; Rabuck, A. D.; Raghavachari, K.; Foresman, J. B.; Cioslowski, J.; J. V. Ortiz,; Baboul, A. G.; Stefanov, B. B.; Liu, G.; Liashenko, A.; Piskorz, P.; Komaromi, I.; Gomperts, R.; Martin, R. L.; Fox, D. J.; Keith, T.; Al-Laham, M. A.; Peng, C. Y.; Nanayakkara, A.; Challacombe, M.; Gill, P. M. W.; Johnson, B.; Chen, W.; Wong, M. W.; Andres, J. L.; Gonzalez, C.; Head-Gordon, M.; Replogle, E. S.; Pople, J. A. *Gaussian 98*, Revision A.11.4; Gaussian, Inc.: Pittsburgh, PA, 2002.
(32) Chertihin, G. V.; Andrews, L. *J. Phys. Chem.* **1995**, *99*, 15 004.
(33) Chertihin, G. V.; Andrews, L. *J. Am. Chem. Soc.* **1995**, *117*, 6402.

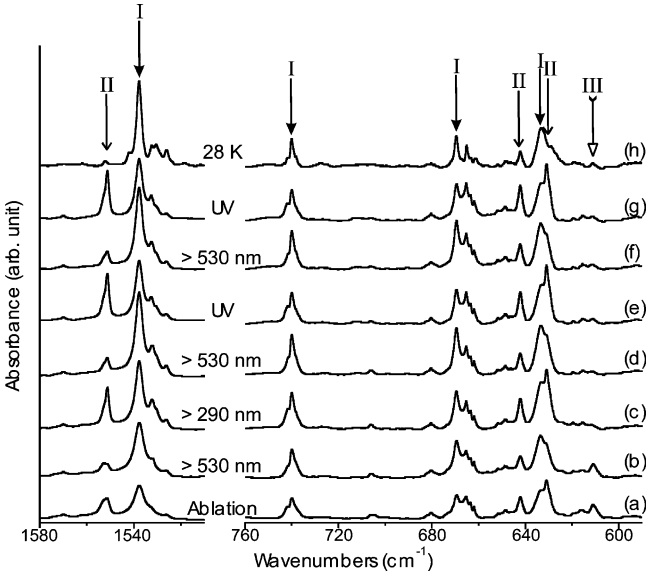

Figure 1. Infrared spectra in the regions of 1510−1580 and 590−760 cm^{-1} for laser-ablated Zr atoms co-deposited with Ar/CH_3F at 7 K. (a) Zr + 0.5% CH_3F in Ar co-deposited for 1 h. (b) After broad-band photolysis with a filter (λ > 530 nm) for 30 min. (c) After broad-band photolysis with a filter (λ > 290 nm) for 30 min. (d) After broad-band photolysis with a filter (λ > 530 nm) for 30 min. (e) After broad-band photolysis with a UV transmitting filter (240 < λ < 380 nm) for 30 min. (f) After broad-band photolysis with a filter (λ > 530 nm) for 30 min. (g) After broad-band photolysis with a UV transmitting filter (240 nm > λ > 380 nm) for 30 min. (h) After annealing to 26 K. I, II, or III stands for the product band group.

absorptions at 1532.4 and 1537.8 cm^{-1}, a reverse effect to that for photolysis with longer wavelength (λ > 530 nm). This photoreversible system is quite persistent: the flip-flop by irradiation with visible and UV light has been demonstrated more than 10 times without noticeable decrease in the absorption intensities.

Similar changes in absorption intensities upon photolysis with visible and UV lights are observed in the region of 590−760 cm^{-1} as shown in Figure 1. The absorptions at 633.5, 655.3, 669.4, 740.0, and 742.0 cm^{-1} increase upon irradiation by visible light (λ > 530 nm), whereas the absorptions at 631.0 and 642.1 cm^{-1} decrease. Irradiation by UV light (240 < λ < 380 nm) reverses this effect. The variations in the region of 590−760 cm^{-1} coincide with those in the region of 1510−1580 cm^{-1}. It is also noticeable that irradiation using a Pyrex filter (λ > 290 nm) results in disappearance of the absorption at 611.0 cm^{-1}, whereas most other product absorptions grow. Once the absorption disappears, it does not reappear in the following irradiation cycles.

On the basis of the behaviors upon photolysis and annealing, the product absorptions are sorted into four groups as listed in Table 1. Group I absorptions increase and decrease upon photolysis with visible (λ > 530 nm) and UV (240 < λ < 380 nm) bands, respectively. They slowly decrease in the process of annealing and show only slight changes up to 28 K. Group II absorptions decrease and increase upon irradiation of the visible and UV lights, the reverse of Group I absorptions. They weaken very fast upon annealing and almost disappear at 28 K. The behaviors of Groups I and II indicate that each group originates from a primary reaction product, and the reaction products are interconvertible in such a manner that an increase in concentration of one product leads to a decrease in concentration of the other product. The absorptions in both Groups I and II increase on Pyrex filter (λ > 290 nm) irradiation as shown in Figure 1. Once the growth is completed, the same type of growth is not observed any further in the following photolyses, even with the same filter. The present results indicate that λ > 290 nm irradiation increases the total concentrations of the two products Group I and II, and once the increase is complete, the total concentrations of the two products remains the same, whereas the mole ratio between the two products varies in following irradiation cycles.

Group III absorptions, including the absorption at 611 cm^{-1}, are observed after reaction of methyl fluoride and laser-ablated metal atoms and even after photolysis with visible light (λ > 380 nm); however, they weaken fast upon photolysis with a Pyrex filter (λ > 290 nm) and eventually disappear. They never reappear in the following processes of photolyses. In other trials, it is confirmed that irradiation of UV light (λ < 380 nm) indeed causes the disappearance, which results in increase of the total concentration of the compounds responsible to Groups I and II.

On the other hand, minor Group IV product absorptions do not show particular changes on irradiation, and they are due to fragments of methyl fluoride, resulting from irradiation by the laser-ablation plume on the Zr target surface. The new product absorptions are summarized in Table 1, including minor products that can be identified by comparison to previous work.[13,20,26]

Neon matrix experiments were also done with CH_3F using a 4.5 K cold window.[30] The product yield was lower: A weak Group III band was observed at 619.9 cm^{-1}. Group I bands appeared at 1604.8, 743.0, 673.5, and 644.0 cm^{-1} and tracked on 530 nm and UV irradiations. There appears to be no evidence for Group II absorptions.

Group I. Most of Group I absorptions are marked with "I" in Figures 1, 2, and 3. The strong absorptions at 1532.4 and 1537.8 cm^{-1} are attributed to the Zr−H stretching mode of the reaction product as described above,[32,33] indicating that C−H insertion by the metal atom readily occurs in the reaction. Another strong absorptions at about 740 cm^{-1} show isotope shifts of −18.5 and −98.2 cm^{-1} on ^{13}C and D substitutions ($^{12}C/^{13}C$ and H/D isotopic frequency ratios of 1.026 and 1.154). Based upon the considerable magnitude of the ^{13}C isotope shift, the absorptions probably arise from the mostly C−Zr stretching mode of the product. The frequency, higher than the expected C−Zr single bond stretching frequency, suggests that the bond between C and Zr is in fact a double bond.

The absorptions at about 669 cm^{-1} show small −4.9 cm^{-1} and large −135.4 cm^{-1} isotope shifts on ^{13}C and D substitutions ($^{12}C/^{13}C$ and H/D isotopic ratios of 1.007 and 1.254), and probably originate from one of the CH_2 bending modes of the product. In the lower frequency region, another strong absorption observed at 633.5 cm^{-1} shows small ^{13}C and D isotope shifts of −1.1 and −26 cm^{-1}, respectively. This band probably arises from the Zr−F stretching mode of the product, which is expected in this region.[21] Consequently, the reaction product most likely contains Zr−H, C═Zr, CH_2, and Zr−F moieties, and the most probable compound that is consistent with the observed vibrational characteristics and also energetically favorable is CH_2═ZrHF.

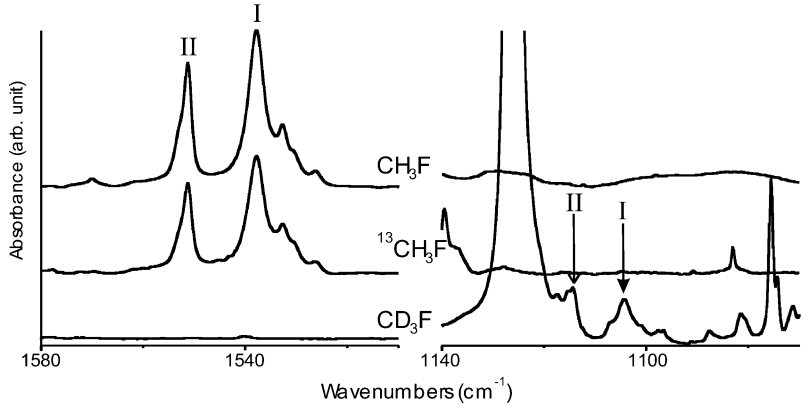

Figure 2. Infrared spectra in the regions of 1510−1580 and 1070−1140 cm^{-1} for laser-ablated Zr atoms co-deposited with methyl fluoride isotopomers diluted in Ar at 7 K. The product group absorptions are identified with I, II, or III.

Table 2. Strong Absorptions Predicted by B3LYP Calculations for Possible Products of Zr + CH_3F Reaction[a]

compound	state	sym	energy	frequencies[a]
CH_3-ZrF	^1A	C_1	1.3[b]	662.9 (110)
CH_3-ZrF	$^3A''$	C_s	−8.1[b,c]	621.1 (136)
$CH_2{=}ZrHF$	^1A	C_1	0.0[b,c]	1605.8 (380), 758.3 (73), 684.6 (129), 651.8 (228)
$CH_2{=}ZrHF$	$^3A''$	C_s	17[b,c]	1610.6 (417), 670.0 (269), 580.7 (58)
$CH-ZrH_2F$	^1A	C_1	70[b]	1696.4 (266), 1619.1 (345), 738.6 (149), 642.6 (100), 618.2 (55), 482.3 (89)
$CH-ZrH_2F$	$^3A''$	C_s	44[b]	1697.5 (264), 1660.5 (456), 675.7 (277), 639.8 (144), 579.2 (56), 478.7 (67)
$CHF{=}ZrH_2$	^1A	C_1	77[b]	1636.8 (260.7), 1601.1 (499), 1387.3 (144), 1269.8 (140), 654.3 (169), 542.6 (103)
$CHF{=}ZrH_2$	$^3A''$	C_s	89[b]	1640.2 (319), 1608.1 (608), 1108.0 (196), 708.9 (113)
CH_2F-ZrH	^1A	C_1	78[b]	1670.2 (337)
CH_2F-ZrH	^3A	C_1	65[b]	1586.3 (453)
$CF-ZrH_3$	^1A	C_1	126[b]	1700.5 (230), 1625.1 (322), 1611.5 (453.2), 1412.9 (533), 675.2 (113), 602.6 (88), 441.0 (105), 409.4 (99)
$CF-ZrH_3$	^3A	C_1	106[b]	1703.4 (205), 1649.4 (516), 1648.7 (516), 1413.8 (319), 609.9 (89), 608.8 (89), 531.2 (254)
$CH{=}ZrHF$	^2A	C_1	0.0[d]	1612.7 (380), 787.1 (57), 638.3 (224), 613.6 (147)
$CH_2{=}ZrF$	$^2A'$	C_s	28[d]	758.8 (68), 649.0 (64), 643.8 (127)
$CF{=}ZrH_2$	^2A	C_1	63[d]	1631.8 (272), 1595.9 (548), 1376.9 (411), 607.4 (167)

[a] Basis 6-311+G(2d,p) and LANL2DZ: frequencies are in cm^{-1}. Shown in parentheses are the expected absorption intensities in km/mol: Only bands with intensities higher than 50 km/mol and frequencies higher than 400 cm^{-1} are listed. [b] Molecular energy (kcal/mol) relative to that of singlet, ground-state $CH_2{=}ZrHF$. [c] MP2 calculations using the SDD pseudopotential and 6-311+G(2d,p) basis set give 3.4, 0.0, and 23.6 kcal/mol, respectively. [d] Molecular energy (kcal/mol) relative to that of $CH{=}ZrHF$.

In an effort to identify the reaction products, DFT calculations were carried out for plausible compounds formed in the reaction of methyl fluoride with Zr atoms. The molecular energies and observable absorptions of the plausible reaction products are summarized in Table 2. On the singlet surface a coplanar $CH_2{=}$ ZrHF structure was about 1 kcal/mol higher energy than the nonplanar ground state, which converged from the planar structure when no symmetry was imposed. The coplanar structure exhibited a 145 cm^{-1} imaginary out-of-plane hydrogen deformation frequency. Geometry optimizations starting from various structures of $CH_2{=}ZrHF$, including ones with the ZrHF group inverted, tilted, or perpendicular with respect to the CH_2 group, all ended up with the singlet ground state structure shown in Figure 4. Furthermore, B3LYP optimizations with LanL2DZ and SDD basis and MP2 calculations all lead to essentially the same structures. However, the relative energies with MP2 are slightly different: $CH_2{=}ZrHF$ (T) is 23.6 kcal/mol higher and CH_3ZrF (T) is 3.4 kcal/mol higher than $CH_2{=}ZrHF$ (S) using SDD. We find that diffuse functions on H (++ set) stabilize the agostic interaction (singlet state) by 0.2 kcal/mol. Since the energies of $CH_2{=}ZrHF$ (S) and CH_3ZrF (T) are close, it is not possible to definitively determine the global minimum energy isomer.

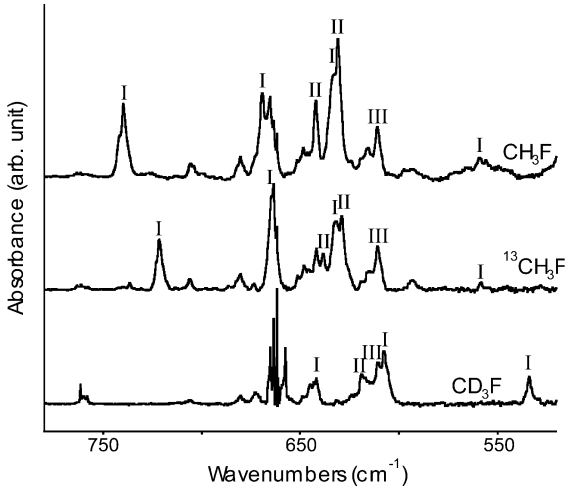

Figure 3. Infrared spectra in the region of 520−780 cm^{-1} for laser-ablated Zr atoms co-deposited with ethylene isotopomers diluted in Ar at 7 K. I, II, or III indicates the product band group.

The observed frequencies of Group I absorptions are compared with the calculated singlet ground-state values in Table 3. The calculated frequencies are high by 68, 18, 16, 18, and 5 cm^{-1} or 4.4, 2.4, 2.4, 2.9, and 0.9%, respectively, which is in

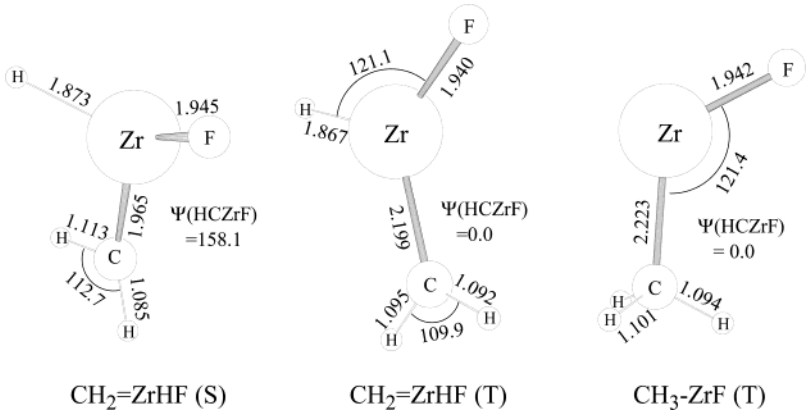

Figure 4. Optimized (B3LYP/6-311+G(2d, p)/LANL2DZ) molecular structures of Zr-methyl fluoride complexes identified in this study. The bond lengths and angles are in Å and degree, and the HCZrF dihedral angles are also shown.

Table 3. Observed and Calculated Fundamental Frequencies (cm^{-1}) of CH_2═ZrHF in the Ground Singlet Electronic State[a]

	CH_2═ZrHF			CD_2═ZrDF			$^{13}CH_2$═ZrHF		
description	obs.	calc.	int.	obs.	calc.	int.	obs.	calc.	int.
ν_1 CH str.		3182.4	1		2353.9	2		3171.6	1
ν_2 CH str.		2887.3	9		2101.9	3		2880.6	9
ν_3 Zr−H str.	1537.8	1605.8	380	1104.3	1142.7	197	1537.8	1605.7	380
ν_4 CH_2 scis.		1329.0	19		1030.8	21		1320.6	19
ν_5 C−Zr str.	740.0	758.3	73	641.8	677.1	48	721.5	738.9	73
ν_6 CH_2 wag	669.4	684.6	129	534.0	535.7	105	664.5	678.9	123
ν_7 Zr−F str.	633.5	651.8	228	607.5	634.7	177	632.4	651.2	227
ν_8 CZrH bend	558.7	562.7	26		424.2	27	558.0	561.7	26
ν_9 CH_2 twist		436.4	27		312.2	10		436.3	27
ν_{10} CH_2 rock		357.7	14		287.0	9		354.1	15
ν_{11} HCZrH distort		258.6	122		191.3	58		258.5	123
ν_{12} CZrF bend		138.6	40		121.8	33		137.2	39

[a] Calculated (B3LYP/6-311+G(2d, p)/LANL2DZ) intensities are in km/mol.

line with previous comparisons of calculated and observed frequencies for stable molecules containing first-row transition metal atoms.[34] The excellent agreement between calculated and observed frequencies confirms the identification of CH_2═ZrHF in the singlet ground state.

Group II. A relatively small number of absorptions belong to Group II as shown in Figures 1, 2, and 3. The strong absorptions at about 1551 cm^{-1} are almost unquestionably attributed to the Zr−H stretching mode of the reaction product, due to the negligible isotope shift by ^{13}C substitution and the large shift of −436 cm^{-1} by D substitution (H/D isotopic ratio of 1.391). Another strong sharp absorption at 631.0 cm^{-1} shows very small isotope shifts of −1.9 and −12 cm^{-1} by ^{13}C and D substitution ($^{13}C/^{12}C$ and H/D isotopic ratio of 1.003 and 1.019), indicating that the absorptions arises from the Zr−F stretching mode of the reaction product. Therefore, the reaction product, the origin of Group II absorptions, contains Zr−H and Zr−F bonds.

Interestingly enough, a molecular species that is energetically favorable and also shows vibrational characteristics consistent with those of Group II absorptions is CH_2═ZrHF in its lowest triplet state, which is 17 kcal/mol higher in energy than that the singlet ground state. This suggests that the photoreversible system could be the singlet and triplet states of CH_2═ZrHF captured by the argon matrix. In Tables 3 and 4 the observed frequencies of Group I and II absorptions are compared with the calculated values for CH_2═ZrHF in the ground singlet and lowest triplet states, and all the observed values of the isotopomers are consistent with the calculated frequencies. On the other hand, it is also possible that Group II absorptions are due to a different argon matrix packing configuration around the singlet state formed by relaxation a triplet state argon complex produced in the photochemical process. This is in accord with observations that triplet CUO binds argon more strongly than singlet CUO.[35] Finally, neon matrix experiments reveal only the ground singlet CH_2═ZrHF species, which shows that the argon matrix cage plays a role in trapping the Group II species.

Photoreversible System. To the best of our knowledge, this is not only the first transition-metal methylidene formed from a transition metal and a simple halomethane but the first photoreversible transition-metal alkylidene system as well. It is also quite interesting that the interconversion may occur through intersystem crossing between the singlet and triplet states: Irradiation with visible light ($\lambda > 530$ nm) transforms the product to the singlet ground state, whereas irradiation with UV light ($240 < \lambda < 380$ nm) forms the triplet state, which is either trapped or relaxed to the singlet state with a different argon packing configuration.

Calculations show that there are substantial differences between the molecular structures in the singlet and triplet states. This substantial variation in the molecular structure of the guest, due to intersystem crossing of the reaction product, is followed by adjustment of the host matrix around the guest accordingly.

(34) Bytheway, I.; Wong, M. W. *Chem. Phys. Lett.* **1998**, *282*, 219.

(35) Andrews, L.; Liang, B.; Li, J.; Bursten, B. E. *J. Am. Chem. Soc.* **2003**, *125*, 3162.

Table 4. Observed and Calculated Fundamental Frequencies (cm^{-1}) of $CH_2{=}ZrHF$ in the Lowest Triplet State[a]

	$CH_2{=}ZrHF$			$CD_2{=}ZrDF$			$^{13}CH_2{=}ZrHF$		
description	obs.	calc.	int.	obs.	calc.	int.	obs.	calc.	int.
ν_1 A′ CH_2 str. (a)		3121.8	5		2312.5	1		3110.3	4
ν_2 A′ CH_2 str. (s)		3040.8	2		2206.7	0		3034.9	2
ν_3 A′ Zr−H str.	1551.3	1610.6	417	1115.3	1145.9	217	1551.3	1610.6	417
ν_4 A′ CH_2 scis.		1366.5	3		1025.4	12		1360.4	2
ν_5 A′ Zr−F str.	631.0	670.0	269	619.0	646.6	188	629.1	668.9	265
ν_6 A′ C−Zr str.	548.9	580.7	58	503.7	532.8	62		570.8	55
ν_7 A′ CZrH bend		534.4	3		413.9	13		528.0	7
ν_8 A′ CH_2 rock		387.5	5		300.2	6		384.7	5
ν_9 A′ CZrF bend		144.7	1		132.0	1		143.7	1
ν_{10} A" CH_2 wag		629.0	37		491.6	24		623.6	68
ν_{11} A" CH_2 twist		226.8	8		160.9	4		226.8	8
ν_{12} A“ HCZrH distort		50.5	68		41.2	38		50.3	68

[a] Calculated (B3LYP/6-311+G(2d, p)/LANL2DZ) intensities are in km/mol.

Table 5. Geometrical Parameters and Physical Constants Calculated for $CH_2{=}ZrHF$ (S), $CH_2{=}ZrHF$ (T), and $CH_3{-}ZrF$ (T)[a]

parameters	$CH_2{=}ZrHF$ (S)	$CH_2{-}ZrHF$ (T)	$CH_3{-}ZrF$ (T)
r(C−H)	1.085, 1.113	1.092, 1.095	1.093, 1.101, 1.101
r(C−Zr)	1.965	2.199	2.223
r(Zr−H)	1.873	1.867	
r(Zr- - -H′)	2.345, 2.968	2.982, 2.948	2.787, 2.787, 2.854
r(Zr−F)	1.945	1.940	1.942
<HCH	112.7	109.9	107.7, 108.0, 108.0
<CZrF	112.9	121.0	121.4
<CZrH	105.8	117.9	
<HZrF	118.6	121.1	
<HCZr	96.5, 149.9	123.5, 126.6	114.4, 109.3, 109.3
Φ(HCZrH)	26.8, −139.3	0.0, 180.0	
Φ(HCZrF)	158.1, −7.9	0.0, 180.0	0.0, 121.2, −121.2
Sym	C_1	C_s	C_s
q(C)[b]	−0.77	−0.80	−0.95
q(H)[b,c]	−0.25, 0.13, 0.09	−0.30, 0.12, 0.12	0.13, 0.13, 0.13
q(Zr)[b]	1.30	1.38	1.12
q(F)	−0.49	−0.53	−0.56
μ[d]	3.58	2.05	2.56
State[e]	^{1}A	^{3}A"	^{3}A"
ΔE[f]	−97	−80	−102

[a] B3LYP/6-311+G(2d,p)/LANL2DZ: Bond lengths and angles are in Å and degrees, respectively. [b] Mulliken atomic charge. [c] Numbers are in the order from the closest one to the metal atom to the farthest. [d] Molecular dipole moment in D. [e] Electronic state. [f] Binding energies in kcal/mol relative to $Zr(^3F) + CH_3F$.

For the new molecular structure frozen in the adjusted matrix environment, the corresponding electronic state is preserved indefinitely by a matrix cage “barrier.”

Zirconium alkylidene complexes have been prepared by reacting $(CpP_2)ZrCl_3$ with alkylating agents: The first such benzylidene complex to be isolated contained a Zr=C bond with 2.024 Å length,[36] which is slightly larger than our computed singlet ground-state Zr=C bond length.

The optimized geometries of $CH_2{=}ZrHF$ in its singlet ground and lowest triplet states are illustrated in Figure 4, and the geometrical parameters are summarized in Table 5. $CH_2{=}ZrHF$ has a C_1 structure in its singlet ground state, where the carbon and metal atom centers serve as trigonal pyramidal apexes but the lowest triplet state has a planar (C_s) structure. It is also noticeable in Figure 4 that unlike in the triplet molecular structure, one of the methylene hydrogen atoms in the singlet molecular structure is located unusually close to the Zr atom in the ground-state structure (<HCZr = 96.5° and r(Zr- - -H) = 2.345 Å), distorting the methylene group. Evidently, there is strong agostic interaction between the metal atom and one of the α-hydrogen atoms in the singlet molecular structure. We note that the C−Zr bond in triplet $CH_2{-}ZrHF$ approaches that of the single bond in $CH_3{-}ZrF$, which suggests that there is little double bond character in triplet $CH_2{-}ZrHF$.

After their initial discovery and subsequent characterization, agostic interactions appear to be quite common, provided a metal has a low-lying empty valence orbital and a C−H bond in reasonable proximity.[37−40] It is implicit that such a bond occurs due to attraction between the electron-deficient metal center and the C−H bond acting as a Lewis base. Studies have revealed interaction energies in the range of 10−15 kcal/mol. The agostic bond forms at the expense of a significant distortion within the ligand including bending at CH_2 and lengthening of the C−H bond. Therefore, it is reasonable to presume that the distorted structure of $CH_2{=}ZrHF$ in its singlet ground state is caused at least partly due to the agostic interaction between the Zr atom and one of the α-hydrogens.

Group III. The weak absorption at 611 cm^{-1} in Figure 1 is clearly observed after deposition and remains even after photolysis with visible light. However, the absorption disappears after near UV irradiation ($\lambda > 290$ nm), and it never reappears in the following course of irradiations. Absorptions essentially at the same frequencies are also observed in the spectra of Zr + CD_3F and Zr + $^{13}CH_3F$ as shown in Figure 3, and they show the same behavior on photolysis. The negligible isotope shifts indicate that the absorption probably arises from the Zr−F stretching mode of a different reaction product, isolated from other vibrational modes involving carbon or hydrogen atoms. Another absorption at 1115.8 cm^{-1}, though much weaker, exhibits the same behavior on photolysis. This band also shows a negligible isotope shift on ^{13}C substitution and a large shift of more than 220 cm^{-1} on D substitution as listed in Tables 1 and 6, suggesting a hydrogen deformation mode.

Earlier studies have shown that the Zr−F stretching frequency of zirconium fluorides generally increases with the Zr valence bonds. For example, the strong absorptions of ZrF_2, ZrF_3, and ZrF_4 are observed at 633.5, 654.8, and 668.0 cm^{-1},[21] and the absorption of ZrF is predicted in a previous study at about 620

(36) Fryzuk, M. D.; Mao, S. S. H.; Zaworotko, M. J.; McGillivray, L. R. *J. Am. Chem. Soc.* **1993**, *115*, 5336.
(37) Bau, R.; Mason, S. A.; Patrick, B. O.; Adams, C. S.; Sharp, W. B.; Legzdins, P. *Organometallics* **2001**, *20*, 4492.
(38) Wada, K.; Craig; B. Pamplin, C. B.; Legzdins, P.; Patrick, B. O.; Tsyba, I.; Bau, R. *J. Am. Chem. Soc.* **2003**, *125*, 7035.
(39) Ujaque, G.; Cooper, A. C.; Maseras, F.; Eisenstein, O.; Caulton, K. G. *J. Am. Chem. Soc.* **1998**, *120*, 361.
(40) Boncella, J. M.; Cajigal, M. L.; Abboud, K. A. *Organometallics* **1996**, *15*, 1905.

Table 6. Observed and Calculated Fundamental Frequencies (cm^{-1}) of CH_3ZrF in the Ground Electronic State ($^3A''$)[a]

	CH_3–Zr–F			CD_3–Zr–F			$^{13}CH_3$–Zr–F		
description	obs.	calc.	int.	obs.	calc.	int.	obs.	calc.	int.
ν_1 A′ CH_3 str.		3078.4	4		2272.3	1		3068.3	4
ν_2 A′ CH_3 str.		2954.0	6		2120.3	1		2950.5	7
ν_3 A′ CH_3 scis.		1415.6	1		1027.1	1		1412.4	1
ν_4 A′ CH_3 deform	1115.8	1158.3	17	890.5	911.9	31	1106.4	1148.6	15
ν_5 A′ Zr−F str.	611.0	621.2	136	610.8	620.2	134	610.9	621.0	136
ν_6 A′ C−Zr str.	489.2	513.7	47		453.2	40		502.9	43
ν_7 A′ CH_3 rock		407.3	18		321.4	7		402.5	19
ν_8 A′ CZrF bend		114.3	4		103.9	4		113.1	4
ν_9 A" CH_3 str.		3012.3	2		2225.0	0		3001.9	3
ν_{10} A" CH_3 scis.		1421.3	8		1031.1	5		1418.1	8
ν_{11} A" CH_2 twist		378.6	10		282.3	6		376.7	9
ν_{12} A“ HCZrF distort		133.3	0		97.5	0		133.2	0

[a] Calculated (B3LYP/6-311+G(2d, p)/LANL2DZ) intensities are in km/mol.

cm^{-1}.[22] Therefore, the low Zr−F stretching frequency of 611 cm^{-1} observed in Figures 1 and 3 suggests that the reaction product responsible for Group III absorptions contains a −ZrF moiety.

One possibility is that the absorption at 611 cm^{-1} arises from ZrF. However, despite considerable efforts, ZrF has not been identified to date in any medium, mainly due to reactivity of the compound.[21,22] Moreover, in the present study, absorptions from zirconium fluorides and methyl radical[13] are not identified, while absorptions from several other radicals containing a C−F bond are observed as listed in Table 1. This is indicative of strong survivability of the C−F bond of methyl fluoride in reaction of the compound with vaporized metal atoms. Finally, the singlet HC≡ZrF molecule was also calculated (HC, 1.091 Å, 1.858 Å, ZrF, 1.980 Å, HCZr, 162.1°, CZrF, 110.3°) and the strongest absorption (Zr−F, predicted at 581 cm^{-1}) is not found in our spectra.

It is notable at this point that a stable compound among the plausible reaction products is CH_3−ZrF in its triplet ground state as shown in Table 2. Geometry optimization with no constraint starting from methyl fluoride with a Zr atom far apart ends up with the structure of CH_3−ZrF (T). Furthermore, the expected vibrational characteristics of CH_3−ZrF (T) are consistent with the observed frequencies as shown in Table 6. The present results argue that in the reaction of Zr atoms and methyl fluoride, CH_3−ZrF is in fact generated.

Our observations also indicate that CH_3−ZrF (T) is readily converted into CH_2═ZrHF by α-H transfer on irradiation by UV light (240 < λ < 380 nm). Alpha-hydrogen elimination is common in organometallic chemistry.[41−43] The total intensity of the Zr−H stretching absorptions from CH_2═ZrH_2 increases about 80%, whereas Group III absorptions disappear on UV irradiation. After the increase in CH_2═ZrHF, the total intensity of the Zr−H stretching absorptions remains essentially the same in the following course of photochemical rearrangements. Once depleted, recovery of the CH_3−ZrF (T) absorptions was not observed even on full arc irradiation (λ > 240 nm) in this study. Apparently, we cannot access an excited methylidene state with a favorable rate of α-H restoration. However, as noticed in Figure 1, Group III bands recover slightly (10−20%) on annealing, probably through a spontaneous C−F bond insertion reaction by Zr on diffusion. In the analogous Ti/CH_3F system, annealing produces more growth in CH_3TiF.[44]

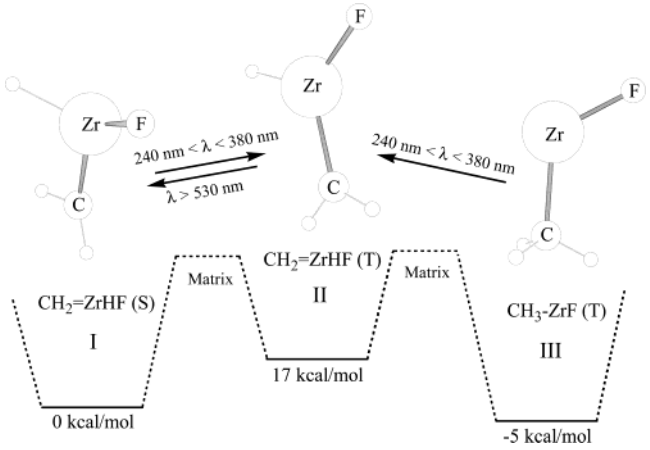

Figure 5. Photoreversible system identified in this study. The singlet and triplet states of CH_2═ZrHF interconvert each other by visible (λ > 530 nm) and UV (240 nm < λ < 380 nm) irradiation. CH_3−ZrF, one of the reaction products, rearranges into CH_2═ZrHF on UV irradiation, increasing concentration of CH_2═ZrHF by 80%. Calculated (B3LYP/6-311+G(2d,p)/LanL2DZ) energies are given for each product: The barriers arise from the argon matrix cage.

The photoreversible transition-metal methylidene system including the Grignard-type product CH_3−ZrF (T) is illustrated in Figure 5 where energies are taken from B3LYP calculations. In reaction of methyl fluoride and laser-ablated Zr atoms, CH_2═ZrHF in its lowest singlet and triplet states and CH_3−ZrF (T) are all generated. Interconversion between the singlet ground and lowest triplet states of CH_2═ZrHF occurs by irradiation of visible (λ > 530 nm) and UV (240 < λ < 380 nm) lights, as described above. Photolysis with UV light (240 nm < λ < 380 nm) transforms CH_3−ZrF (T) into CH_2═ZrHF, increasing the total concentration of CH_2═ZrHF. It is likely that UV irradiation promotes α-H shift on the triplet surface and intersystem crossing to the lower energy singlet state follows. Finally, the triplet methylidene formed here may in fact relax to give a different argon matrix configuration around the singlet.

Group IV. The product absorptions whose intensities remain practically unchanged in the course of photolyses are sorted into Group IV. Among them, the absorption at 1161.9 cm^{-1} due to the C−F stretching absorption of CH_2F radical, is the strongest.[13,26] In solid neon this band shifted to 1165.1 cm^{-1}.

(41) Green, M. L. H. *Pure Appl. Chem.* **1978**, *50*, 27.
(42) Schrock, R. R. *Acc. Chem. Res.* **1979**, *12*, 98.
(43) Crabtree, R. H., *The Organometallic Chemistry of the Transition Metals*; Wiley and Sons: New York, 2001; p 190.
(44) Cho, H.-G.; Andrews, L. *J. Phys. Chem. A* **2004**, *108*, 6294.

The identified reaction products are consistent with those from vacuum UV photolysis of methyl fluoride as reported in a previous study by Jacox and Milligan.[13] This result indicates that laser-ablation of transition metals produces vacuum UV light. Apparently the reaction products responsible for Group IV absorptions do not affect by any means the interconversions between the singlet and triplet states of CH_2═ZrHF and transformation of CH_3−ZrF (T) to CH_2═ZrHF in sequential photolyses. The photoreactions are most likely unimolecular in the matrix.

Conclusions

Reactions of laser-ablated Zr atoms with methyl fluoride in excess argon have been carried out during condensation at 7 K. The product infrared absorptions are sorted into four groups on the basis of the behaviors upon photolysis and annealing. Group I reversibly increases and decreases on visible ($\lambda > 530$ nm) and UV (240 nm $< \lambda <$ 380 nm) irradiations, whereas Group II shows the reverse trend. Spectroscopic evidence and DFT calculations indicate that Group I is the ground singlet state CH_2═ZrH_2 and Group II is either triplet CH_2═ZrH_2 frozen in the matrix or the singlet with a different argon packing configuration. The molecular structures of CH_2═ZrHF in its ground singlet and lowest triplet states are substantially different, and there is evidence for agostic interaction between the metal atom and one of the α-hydrogen atoms in the ground singlet state.

Group III is attributed to a Grignard type compound CH_3−ZrF in its triplet ground state, whose molecular energy is the low among the plausible reaction products. CH_3−ZrF (T) is readily converted via hydrogen migration into CH_2═ZrHF on irradiation by UV light, increasing the total concentration of CH_2═ZrHF by 80%. Other reaction products are also identified in the infrared spectra, such as CH_2F radical, consistent with the vacuum UV photolysis of methyl fluoride in the laser-ablation process.[13] As shown in this study, transition-metal methylidenes formed from halomethanes not only reveal greatly interesting properties, but also serve as a model systems to investigate the nature of coordination chemistry and agostic interactions.

Acknowledgment. We gratefully acknowledge financial support for this work from N.S.F. Grant CHE 00-78836 and sabbatical leave support (H.-G.Cho) from the Korea Research Foundation (KRF-2003-013-C00044).

JA0486115